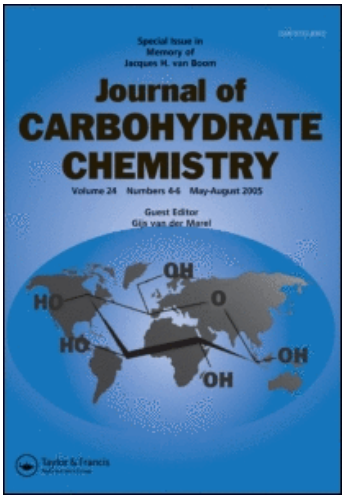

Journal of Carbohydrate Chemistry
Publication details, including instructions for authors and subscription information:
http://www.informaworld.com/smpp/title~content=t713617200

Three-Dimensional Structure of Fucosyllactoses in an Aqueous Solution

Yasuko Ishizuka; Tadashi Nemoto; Masako Fujiwara; Ken-ichi Fujita; Hiroshi Nakanishi

To cite this Article Ishizuka, Yasuko , Nemoto, Tadashi , Fujiwara, Masako , Fujita, Ken-ichi and Nakanishi, Hiroshi(1999) 'Three-Dimensional Structure of Fucosyllactoses in an Aqueous Solution', Journal of Carbohydrate Chemistry, 18: 5, 523 — 533
To link to this Article: DOI: 10.1080/07328309908544016
URL: http://dx.doi.org/10.1080/07328309908544016

J. CARBOHYDRATE CHEMISTRY, 18(5), 523–533 (1999)

THREE-DIMENSIONAL STRUCTURE OF FUCOSYLLACTOSES IN AN AQUEOUS SOLUTION[1]

Yasuko Ishizuka,[a]* Tadashi Nemoto,[a] Masako Fujiwara,[b]
Ken-ichi Fujita[b] and Hiroshi Nakanishi[a]

[a]National Institute of Bioscience and Human Technology, 1-1 Higashi,
Tsukuba, Ibaraki 305-8566, Japan,
[b]JEOL Datum Ltd., 3-1-2 Musashino, Akishima, Tokyo 196-8558, Japan

Received September 16, 1998 - Final Form February 8, 1999

ABSTRACT

^{1}H and ^{13}C NMR spectra of four fucosyllactoses were analyzed and interresidual NOEs were detected in solution. Several interresidual NOE cross peaks between non-direct-bonding pyranoses were obtained in common with trisaccharides including fucose. Three-dimensional (3D) structures of the four saccharides were simulated with DADAS90 software using distance constraints estimated by NOE intensity. Results suggest approximate C2 rotating symmetry in the 3D 3,2'-difucosyllactose structure.

INTRODUCTION

To detect the interesting three-dimensional (3D) structural changes in receptor saccharides interacting with hemagglutinin, the 3D molecular structure must be studied in solution. Saccharides, including fucose, are important in the recognition reaction on the cell surface, particularly in blood-type saccharides.[2-5] Since fucose has a methyl group in

its residue, the fucosyl residue is considered to be a typical, relatively hydrophobic pyranose moiety in polysaccharide chains.

We studied the 3D structure of four fucosyllactoses: 3-fucosyllactose (**1**), 2'-fucosyllactose (**2**), 3,2'-difucosyllactose (**3**), and 3-fucosyllactotetraose (**4**), in D_2O solution using NMR spectroscopy. Three saccharides, **1**, **3**, and **4**, have a composition unit of 3-fucosyllactose in their molecular structure, and two saccharides, **2** and **3**, have the other composition unit of 2'-fucosyllactose. The question is whether the steric saccharide structure conserves the steric structures of the composition unit. Two isomers (α and β anomers) exist in an aqueous solution. It is important to know the differences in the steric structures of these anomers. We compared the interresidual NOE correlational peaks of these four saccharide molecules and simulated 3D structures with DADAS90 software using distance constraints estimated from the intensity of NOE cross peaks.

EXPERIMENTAL PROCEDURE

Four commercially available fucosyllactoses; β-D-galactopyranosyl-(1→4)-[α-L-fucopyranosyl-(1→3)]-D-glucopyranose (**1**), α-L-fucopyranosyl-(1→2)-β-D-galactopyranosyl-(1→4)-D-glucopyranose (**2**), α-L-fucopyranosyl-(1→2)-β-D-galactopyranosyl-(1→4)-[α-L-fucopyranosyl-(1→3)]-D-glucopyranose (**3**), and β-D-galactopyranosyl-(1→3)-(2-acetamido-2-deoxy-β-D-glucopyranosyl)-(1→3)-β-D-galactopyranosyl-(1→4)-[α-L-fucopyranosyl-(1→3)]-D-glucopyranose (**4**) (Seikagaku Co. Tokyo, Japan) were used as samples of NMR measurement without further purification. ^1H and ^{13}C NMR spectra were recorded at 298 or 288 K with a Bruker DMX 750 (750.13 MHz for ^1H and 188.83 MHz for ^{13}C) and DMX 500 spectrometers (500.13 MHz for ^1H and 125.77 MHz for ^{13}C) in D_2O solutions. The concentration of NMR samples was 3.0-15.4 mM. External sodium-2,2-dimethyl-2-silapentonate-d_4 (DMSP) was used as a reference.

Simulation was done by DADAS90 running on SGI Indigo2. Visualizing and RMSD calculation were done using VIEWER and MOLGEM software. All software came from a Molskop software package supplied by JEOL Ltd.

Pyranose Ring.

To assign proton signals, pyranose rings were labeled A, B, C, and D from the reducing terminal to the non-reducing terminal. The fucose residue binding to the reducing terminal was labeled E and the fucose residue binding to the pyranose ring next to the reducing terminal was labeled F.

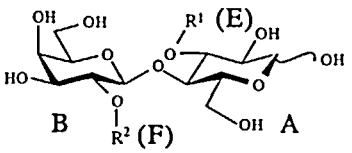

1 R^1 = Fuc, R^2 = H

2 R^1 = H, R^2 = Fuc

3 R^1 = R^2 = Fuc

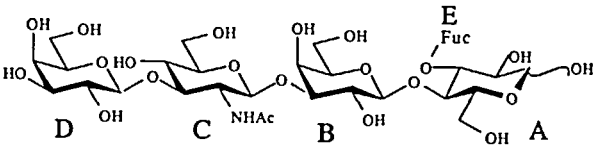

4

Fuc =

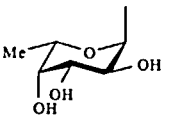

RESULTS AND DISCUSSION

^{1}H NMR Spectra Characteristics.

In common with the three fucosyllactoses with an E fucosyl residue, the E1 proton in the lowest field was observed as two signals (Figure 1) that did not fuse at 368 K. Therefore these E1 signals were not caused by the existence of exchange systems. The reducing terminal in these four solutions has two anomeric isomers. The intensity ratio of the two E1 signals coincides with the intensity ratio of the two A1 signals, A1α and A1β. Since β anomer was the major component in the solution, as for 3, a large E1 signal at 5.462 ppm was estimated to be the E1 signal of β anomer, and the small E1 signal at 5.406 ppm was from one α anomer. NOE correlational peaks were detected between A3β and E1 at 5.462 ppm and between A3α and the second E1 at 5.406 ppm, indicating additionally that the two E1 signals in the lowest field are caused by the two anomeric isomers of the reducing terminal.

Chemical shift differences in the two E1 signals are considerably large (Table 1). The proton signals of the pyranose ring second from the reducing terminal show anomeric differences, but differences shown in Table 1 are several times larger than previously reported.[7,8] In addition to E1, another relatively large splitting of F5 signals occurred (Figure 1). Methyl F6 and E6 signals are isolated doublets in the highest field, and signal splitting is clearly detected despite the small differences. The chemical shift differences also occurred in F5, F6, and E6 splitting (Table 1). Although these splittings could not be explained as originating in the same way as E1 splitting, it is reasonable to consider that at least essentially anomeric differences exist in chemical shifts in fucose next to the reducing terminal and is a major reason for splitting.

^{1}H and ^{13}C Signal Assignment.

^{1}H and ^{13}C signals of the four fucosyllactoses were assigned based on detailed analyses of 1D HOHAHA, 2D TOCSY, DQF-COSY, and NOESY spectra. Inverse CH-

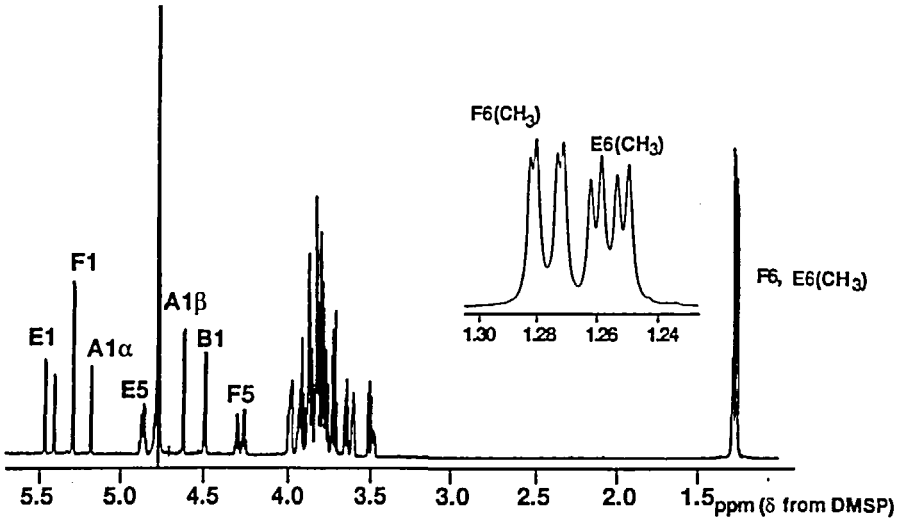

Figure 1. ^{1}H NMR spectrum of 3,2'-difucosyllactose **3** observed with a DMX750 spectrometer in D_2O solution at 298 K.

Table 1. Chemical shift differences in ^{1}H signals of fucose (ppm).

	1	2	3	4
E1	0.0573	-	0.0564	0.0568
F1	-	0.0039	0	-
F5		0.0304	0.0379	
E6	0.0056	-	0.0037	0.0058
F6	-	0.0032	0.0018	-

COSY spectra were used to determine the chemical shifts of A6, B6, C6, and D6 protons and all ^{13}C signals (Tables 2-9). Anomeric differences in the chemical shifts of E1 in ^{13}C spectra were also observed (Tables 6, 8, and 9).

Interresidual NOE.

NOE correlational peaks were obtained in 2D NOESY and ROESY spectra. Several experiments with different mixing times from 300 ms to 1 s for NOESY spectra and a few experiments with different spin lock conditions for ROESY spectra were conducted. Among observed NOE correlational peaks with roughly defined intensity in four classes (Table 10), strong and medium intense NOE correlational peaks were common

Table 2. ^{1}H Signals of 3-fucosyllactose, **1**, (ppm from DMSP).

Residue	H-1	H-2	H-3	H-4	H-5	H-6a	H-6b
Aα	5.192	3.776	3.953	3.812	3.978	3.876	3.900
Aβ	4.662	3.479	3.786	3.883	3.596	3.977	3.824
Bα	4.441	3.499	3.661	3.909	3.601	3.719	3.753
Bβ	4.441	3.491	3.657	3.909	3.601	3.719	3.753
Eα	5.393	3.811	3.977	3.802	4.839	1.198	
Eβ	5.450	3.803	3.972	3.802	4.826	1.193	

Table 3. ^{1}H Signals of 2'-fucosyllactose, **2** (ppm from DMSP).

Residue	H-1	H-2	H-3	H-4	H-5	H-6a	H-6b
Aα	5.235	3.598	3.810	3.735	3.918	3.820	3.901
Aβ	4.646	3.304	3.594	3.738	3.488	3.956	3.778
B	4.533	3.680	3.716	3.901	3.878	3.820	3.745
Fα	5.317	3.822	3.800	3.824	4.266	1.237	
Fβ	5.321	3.822	3.800	3.824	4.236	1.233	

Table 4. ^{1}H Signals of 3,2'-difucosyllactose, **3** (ppm from DMSP).

Residue	H-1	H-2	H-3	H-4	H-5	H-6a	H-6b
Aα	5.189	3.782	3.918	3.862	3.936	3.844	3.933
Aβ	4.634	3.493	3.714	3.880	3.467	3.816	3.995
Bα	4.504	3.643	3.869	3.878	3.598	3.725	3.761
Bβ	4.501	3.640	3.869	3.878	3.598	3.725	3.761
Eα	5.406	3.814	3.985	3.831	4.885	1.257	
Eβ	5.462	3.815	3.985	3.831	4.871	1.253	
Fα	5.293	3.815	3.805	3.819	4.304	1.277	
Fβ	5.293	3.815	3.805	3.916	4.266	1.275	

Table 5. ^{1}H Signals of 3-fucosyllactotetraose, **4** (ppm from DMSP).

Residue	H-1	H-2	H-3	H-4	H-5	H-6a	H-6b	CH_3 (N-Acetyl)
Aα	5.188	3.770	3.935	3.861	3.972	3.883	3.953	
Aβ	4.660	3.469	3.777	3.877	3.603	3.971	3.819	
B	4.426	3.512	3.734	4.109	3.588	3.906	3.793	
C	4.717	3.920	3.819	3.591	3.486	3.759	3.778	2.034
D	4.457	3.530	3.651	3.916	3.714	3.707	3.757	
Eα	5.383	3.809	3.961	3.794	4.846	1.173		
Eβ	5.439	3.804	3.961	3.794	4.846	1.167		

Table 6. ^{13}C Signals of 3-fucosyllactose, **1** (No Reference, 104.66 ppm for B1).

Residue	C-1	C-2	C-3	C-4	C-5	C-6
Aα	95.02	75.65	77.57	74.89	73.81	62.54
Aβ	98.85	78.38	79.85	75.54	78.21	62.65
B	104.66	74.01	75.35	71.17	77.83	64.44
Eα	101.12	70.90	72.17	70.90	69.29	17.93
Eβ	101.50	70.90	72.17	70.90	69.29	17.93

Table 7. ^{13}C Signals of 2'-fucosyllactose, **2** (No Reference, 103.13 ppm for B1).

Residue	C-1	C-2	C-3	C-4	C-5	C-6
Aα	94.67	74.17	74.17	78.75	73.21	62.91
Aβ	98.77	76.83	77.14	78.75	78.23	63.07
B	103.13	79.13	78.11	72.04	76.51	63.98
F	102.24	71.00	72.49	74.56	69.69	18.13

Table 8. ^{13}C Signals of 3,2'-difucosyllactose, **3** (ppm from DMSP).

Residue	C-1	C-2	C-3	C-4	C-5	C-6
Aα	94.93	75.62	77.60	75.50	73.62	62.70
Aβ	98.81	78.46	79.98	75.50	78.46	62.78
Bα	103.04	79.22	76.46	71.63	77.75	64.36
Bβ	103.01	79.22	76.46	71.61	77.75	64.32
Eα	101.29	72.59	72.12	74.85	69.40	18.23
Eβ	101.17	72.56	72.05	74.88	69.47	18.27
Fα	102.19	71.09	70.94	74.54	69.74	18.29
Fβ	102.19	71.09	70.89	74.54	69.71	18.29

Table 9. ^{13}C Signals of 3-fucosyllactotetraose, **4** (No Reference, 104.32 ppm for B1).

Residue	C-1	C-2	C-3	C-4	C-5	C-6	CH_3 (N-Acetyl)
Aα	94.68	79.56	77.22	74.72	73.48	62.26	
Aβ	98.37	78.04	75.19	74.77	77.96	62.36	
B	104.32	73.19	84.09	70.79	77.11	63.01	
C	105.24	57.23	84.49	70.87	77.69	63.68	24.78
D	106.11	73.19	74.96	71.01	77.83	64.16	
Eα	101.10	70.45	71.74	74.43	68.95	17.70	
Eβ	101.02	70.45	71.74	74.43	68.95	17.70	

Table 10. Detected interresidual NOEs

	1	2	3	4		1	2	3	4
E1-A2(α)	w	x	-	w	B1-A2(α)	m-vw	-	-	-
E1-A2(β)	w-vw	x	-	-	B1-A3(α)	w-vw	w	w	-
E1-A3(α)	m*	x	m-w*	s-m*	B1-A3(β)	-	vw	vw	-
E1-A3(β)	s*	x	s*	s*	B1-A4(α)	s*	s*	s*	s*
E1-A4(β)	w	x	-	w-vw	B1-A4(β)	s*	s*	s*	s*
E1-A6(α)	w	x	-	w-vw	B1-A5(β)	-	vw	-	-
E1-B3(α)	-	x	w	-	B1-A6(α)	m	s	s	-
E5-A2(α)	w-vw	x	-	-	B1-A6(β)	s-m	s-m	s-m	m-w
E5-A3(α)	w-vw	x	w-vw	-					
E5-A4(β)	-	x	vw	-	F1-B2	x	s*	s*	x
E5-A6(α)	w-vw	x	-	-	F1-B3	x	-	w	x
E5-A6(β)	-	x	-		F5-A3(β)	x	-	vw	x
E5-B2	s	x	s	s	F5-A4(α)	x	-	w	x
E5-B6	w-vw	x	m-w	-	F5-A4(β)	x	-	w-vw	x
E6-A4(β)	w-vw	x	-	-	F5-A5(α)	x	m	s	x
E6-A5(β)	-	x	-	vw	F5-A5(β)	x	m-w	s	x
E6-A6(α)	-	x	-	w	F5-A6(α)	x	m	-	x
E6-A6(β)	w	x	-	-	F5-A6(β)	x	w	w-vw	x
E6-B2	s-w	x	s-m	m	F5-B2(α)	x	w	w-vw	x
E6-B3	vw	x	-	-	F5-B2(β)	x	w	vw	x
E6-B6	m-w	x	-	-	F6-A3(β)	x	vw	w-vw	x
					F6-A5(β)	x	vw	w	x
					F6-A6(α)	x	-	w-vw	x

s: strong, m: medium, w: weak, vw: very weak; s-m: Some peaks were strong and others medium in 2D spectra. -: not observed, x: no possibility; *: *O*-glycosyl bond.

to both anomers α and β with these four fucosyllactoses. Several anomeric differences in weak NOE correlational peaks were obtained, indicating differences in the 3D structure of these anomers are not so great. Strong and medium intense NOE correlational peaks caused by the E residue were common in **1**, **3**, and **4** (Table 10). Strong and medium intense NOE correlational peaks caused by the F residue were common in **2** and **3**. These facts suggest that the 3D structure of the trisaccharides including E or F residues are very similar.

3D Fucosyllactose Structure.

To construct the 3D saccharide structure, we conducted simulations using the DADAS90 program, determining the best-fit structures with non-constraint violation and low RMSD among the resulting 100 structures from 100 initially random structures (Figure 2). Strong and medium intense NOEs (Table 10) were used to estimate distance constraints for the simulation. Comparing Figures 2a to 2c, the steric structure of **1** (a) was conserved in the steric structure of **3** (c). The steric structure of **2** was conserved in the steric structure of **3** (Figures 2b and 2c). The rough conservation of the steric structure of **1** was also seen in the steric structure of **4** (Figure 2d). The 3D structure of **3** thus presents two typical types of trisaccharide units, including one fucose. Torsion angles relating three glycosyl bonds of **3** are shown in Figure 3. Similar torsion angles were obtained for the corresponding *O*-glycosyl bond for the other three samples **1**, **2**, and **4**. Figure 4 shows a view of simulated structures of **3**, and saccharide **3** has approximate C2 rotating symmetry. Similar pseudo-C2 symmetry was reported for a tetrasaccharide composing the Lewis Y and Lewis b antigen.[9,10] A tetrasaccharide in which two fucosyl residues are connected to hydroxyl groups next to the *O*-glycosyl bond appears to result in this approximate C2 symmetry.

Distance from Anomeric Hydroxyl Group and Anomeric Difference of E1 and F5 Signals.

The simulated structure of **3** made it clear that the distance between E1 proton (E1H) and A1 oxygen (A1O) is ca. 4.3 Å for the α anomer and 5.5 Å for the β anomer. The steric difference between the two isomers is clear. We also found that the distance between F1H and A1O was 7.3 Å for the α anomer and 9.5 Å for the β anomer. If a considerably hard network of hydrogen bonds exists between solvent water and saccharide molecules, the anomeric difference in the chemical shift of E1 may be caused by differences in the distance from E1H to A1O in both anomers. For F1 signals, the distance from F1H to A1O is too long to maintain the network of hydrogen bonds in both anomers, so signal splitting of F1 caused by the two anomers was not observed in the spectra of **3**. Actually anomeric differences in E1 signals observed with **1**, **3**, and **4** were up to 10 times the difference in F1 of **2** (Table 1).

The relatively large difference in the chemical shift of the two F5 signals (Table 1) may be explained by two factors: the distance between F5H and A1O and the large anomeric difference in distance. In simulated structures of **3**, the distance between F5H and A1O was dispersed between 4.3 Å and 6.5 Å with a large anomeric difference. Moderate differences in the chemical shift of F6 signals (Table 1) are also explained by

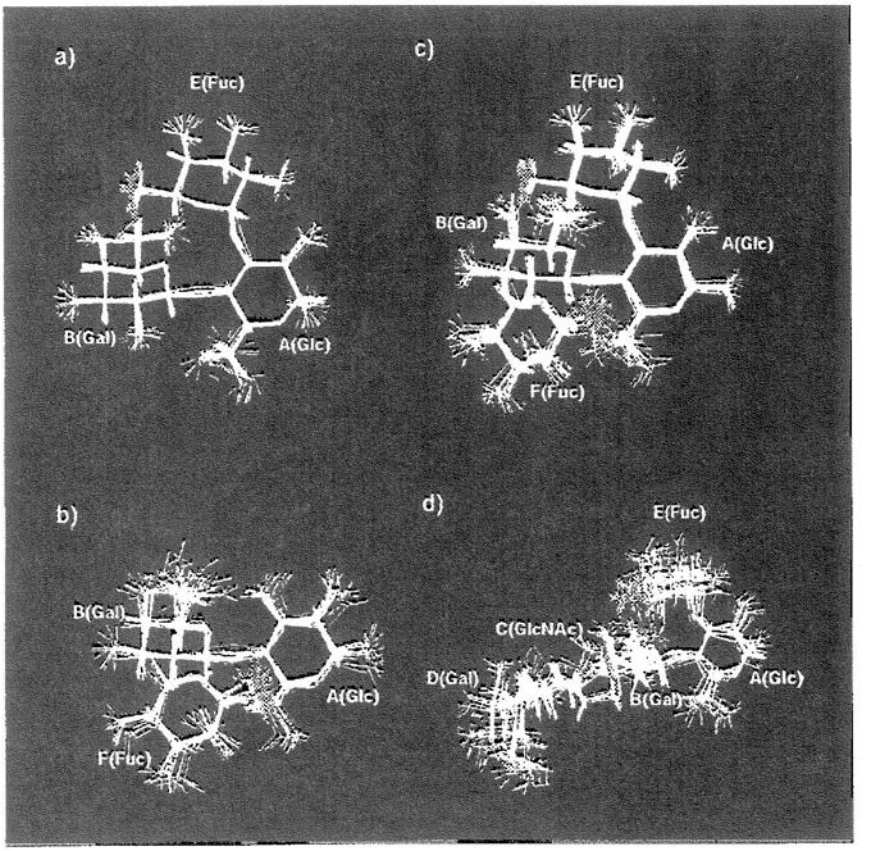

Figure 2. Best-fit structures simulated with DADAS90 software using distance constraint and van der Waals radii. a) **1**, b) **2**, c) **3**, and d) **4**.

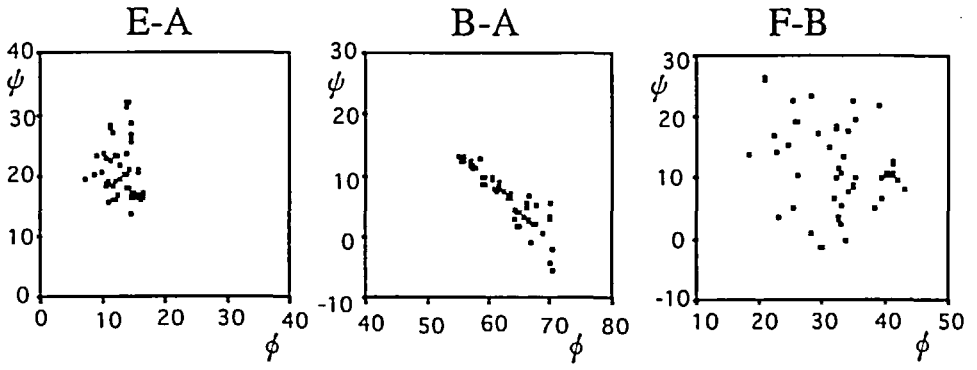

Figure 3. Torsion angles of *O*-glycosyl bond in best-fit structures 3β simulated with DADAS90. Almost the same torsion angles were obtained for 3α. φ denotes torsion angle E1H-E1C-E1O-A4C and ψ denotes torsion angle E1C-E1O-A4C-A4H for the first figure.

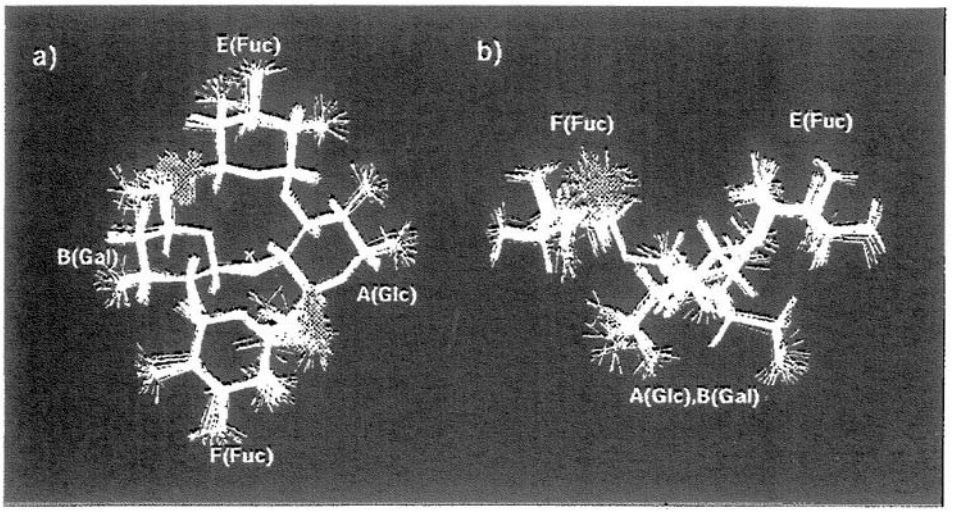

Figure 4. Best-fit structures **3** seen from two different directions. a) These appear to have an approximate C2 rotating axis at x. b) C2 rotating axis in the vertical line on the sheet.

similar factors for F5 signals. The distance from F6H to A1O was dispersed between 4.2 Å and 7.5 Å with a large anomeric difference. The distance between E5H and A1O was longer than that between F5H and A1O, and the anomeric difference in distance was not as large as for F5H. These facts were responsible for no splitting in E5 signals. For the splitting of E6 signals, the alternative reason must be considered. Chemical shift differences in E6 signals were larger than those of F6 signals, but, the distance between E6H and A1O was longer than 8 Å with small anomeric differences.

CONCLUSIONS

^{1}H and ^{13}C NMR spectra of four fucosyllactoses (**1-4**) were analyzed, and interresidual NOEs were detected in an aqueous (D_2O) solution. Several interresidual NOEs between non-direct bonded pyranoses were obtained in common with trisaccharide units including fucose residue. 3D structures of the four saccharides were simulated with DADAS90 software using distance constraints based on NOE intensity. Approximate C2 rotating symmetry appears to exist in the structure of **3**, and the anomeric difference in the chemical shift of E1 and F5 protons in these saccharides is explained by the relationship of the distance from the anomeric hydroxyl group.

REFERENCES AND NOTES

1. Presented at *XIXth International Carbohydrate Symposium*, San Diego, USA, Aug. 9-14, 1998.
2. H. C. Gooi, T. Feizi, A. Kapadia, B. B. Knowles, D. Solter and M. J. Evans, *Nature*, **292**, 156 (1981).
3. A. Mizoguchi, S. Takasaki, S. Maeda and A. Kobata, *J. Biol. Chem.*, **259**, 11949 (1984).
4. E. Spooncer, M. Fukuda, J. C. Klock, J. E. Oates and A. Dell, *J. Biol. Chem.*, **259**, 4792 (1984).
5. G. Walz, A. Aruffo, W. Kolanus, M. Bevilacqua and B. Seed, *Science*, **250**, 1132 (1990).
6. Commercially available software for simulating 3D structure using three types of constraints, distance, van der Waals radii, and torsion angle. This software was proposed for structural analysis of proteins in which only amide bonding dihedral angles were used as variables in simulations. W. Braun and N. Go, *J. Mol. Biol.*, **186**, 611 (1985).
7. J. Berg, D. Roman, H. van Halbeek and J. F. G. Vliegenthart, *Carbohydr. Res.*, **174**, 23 (1988).
8. Y. Ishizuka, unpublished data on lactose.
9. A. Geyer, G. Hummel, T. Eisele, S. Reinhardt and R. R. Schmidt, *Chem. Eur. J.*, **2**, 981 (1996).
10. A. Geyer, S. Reinhardt and R. R. Schmidt, *XIXth International Carbohydrate Symposium*, AP022, San Diego (1998).